Article

Bond Behavior of Deformed Bamboo (*Bambusa vulgaris*) Embedded in Fly Ash Geopolymer Concrete

Dinie Awalluddin [1], Mohd Azreen Mohd Ariffin [1,*], Yusof Ahmad [1], Nor Fazlin Zamri [1], Mohd Mustafa Al Bakri Abdullah [2,3], Rafiza Abd Razak [2], Han-Seung Lee [4] and Jitendra Kumar Singh [4]

1   School of Civil Engineering, Faculty of Engineering, Universiti Teknologi Malaysia, Skudai, Johor Bahru 81310, Malaysia; mdkhalis2@live.utm.my (D.A.); a-yusof@utm.my (Y.A.); fazlinzm@gmail.com (N.F.Z.)
2   Centre of Excellence Geopolymer and Green Technology (CEGeoGTech), Universiti Malaysia Perlis (UniMAP), Perlis 01000, Malaysia; mustafa_albakri@unimap.edu.my (M.M.A.B.A.); rafizarazak@unimap.edu.my (R.A.R.)
3   Faculty of Chemical Engineering Technology, Universiti Malaysia Perlis (UniMAP), Perlis 01000, Malaysia
4   Department of Architectural Engineering, Hanyang University, 1271 Sa 3-dong, Sangnok-gu, Ansan 15588, Korea; ercleehs@hanyang.ac.kr (H.-S.L.); jk200386@hanyang.ac.kr (J.K.S.)
*   Correspondence: mohdazreen@utm.my

Abstract: As the fastest growing plant with high tensile strength, bamboo provides an excellent alternative material to replace steel reinforcement in a concrete structure. However, the bond of bamboo embedded in concrete is very poor due to its surface properties and swell–shrink behaviors, especially when embedded in ordinary Portland cement concrete (OPCC). Thus, this paper presents the experimental investigation on the bond performance of deformed and undeformed bamboo species of *Bambusa vulgaris* strips embedded in fly ash geopolymer concrete (FAGC). Undeformed bamboo strips with and without nodes were compared to deformed bamboo strips in a corrugated and Galvanized Iron (G.I) rolled wired form in the pull-out test to study the mechanical interlocking effect on the bond performance of bamboo strips embedded in concrete. The groove on the corrugated bamboo strip was made using a router machine, while the wired bamboo was produced by wrapping the G.I wire along the bamboo strip. The difference in groove and wire spacing of the deformed bamboo strip on the bond strength was also observed. The result showed that the geometry of the bamboo strip had a significant effect on the bond performance, with the deformed bamboo strip outperforming the undeformed bamboo strip. In addition, the utilization of FAGC could also reduce the moisture absorption by the bamboo strip. Thus, these results showed that using bamboo strips in FAGC is feasible, contributing to a promising approach for full utilization of bamboo and industrial waste products such as fly ash as construction materials.

Keywords: bamboo; fly ash; geopolymer; pull-out; bond

1. Introduction

Several studies on natural reinforcing materials such as wood [1], palm stalk [2], jute [3], and raffia palm [4] have been carried out. Attention is gradually being focused on exploring the use of low-energy-consumption and low-cost-substitute construction materials. One of the possibilities that has the most economic potential for such substitutions is using bamboo as an alternative reinforcement in concrete. Bamboo is a member of the grass family [5–7] that ranges from small to larger diameter, and there are more than a hundred species in the world. As one of the fastest-growing plants on Earth, bamboo has many species that range in size from a few centimeters to many meters tall. Some giant bamboo species can generally reach their full height up to 30 m in a period of 2 to 4 months [8]. The growth rate of bamboo can also reach as high as 20 cm to 100 cm per day. It was found that the tensile strength of some species of bamboo is relatively high and can reach 581 MPa [9]. In fact, the ratio of tensile strength to the specific weight of bamboo is six times greater than

that of steel. Thus, bamboo offers an attractive opportunity to replace steel as a reinforcing material in reinforced concrete structures.

A few studies have been carried out on using raw bamboo as reinforcing materials to replace conventional steel. In 1950, Glenn [10] researched the use of natural raw bamboo as reinforcement in concrete structures using ordinary Portland concrete (OPC). Using small-diameter bamboo strips, he demonstrated that although the application is feasible in principle, there were disadvantages regarding shrinking and swelling due to existing moisture from internal and external concrete due to the hygroscopic behavior of bamboo. In addition, OPC concrete usually has a higher moisture absorption rate due to less compacted structures. The difficulty associated with resistance on raw bamboo embedded in OPC concrete is that it absorbs moisture from the surrounding environment through uncompacted structures and fine cracks in OPC concrete. This results in swelling of the bamboo. Swelling also occurs when there is sufficient time for water to reach the bamboo before the concrete cures. The moisture is absorbed by the bamboo microstructure, which induces the expansion of the bamboo reinforcement and promotes internal local stress in the concrete surrounding the bamboo. Over an extended period, the consequences are the degradation of bamboo, and brittle splitting failure in concrete can result in sudden collapse [11].

The fundamental problem of bamboo as a reinforcing bar in reinforced concrete structures is the weak bond between the bamboo and concrete. The assumption that the perfect bond exists in the design of bamboo-reinforced concrete becomes unrealistic due to the weak bamboo-concrete bond. Many researchers have improved the bamboo–concrete bond, but it is unclear how these improvements can affect bamboo-reinforced concrete structures' behavior. Previous researchers have summarized that the structures failed under low loads due to poor bamboo–concrete bonds [12,13], which can be attributed to two factors. First, the bamboo strips absorb the water from the concrete and cause bamboo bars' expansion inside the concrete. Upon the loss of moisture, the strips shrink and lose contact with the concrete surface. Second, the smooth condition of the bamboo surface that can minimize friction allows the bamboo strips to slip without developing a strong bond.

To tackle the swell–shrink problems, a few research studies have been conducted by using coating material and epoxies. A study on bamboo coating was performed using Sikadur 32-gel adhesive. Ghavami [14] reported the same output where the bond strength of uncoated bamboo embedded in lightweight OPC concrete was 0.52 MPa, while bamboo coated with Sikadur-32 gel was 3.25 MPa, a total increment of 430%. They also reported that the combination of asphalt (Negrolin) and sand coating resulted in 0.73 MPa of bond strength [9]. Studies on the other coating materials were also conducted using synthetic resin and synthetic rubber surface adhesive. Terai and Minami [15] reported that the bond value of uncoated bamboo was 0.66 MPa and the treatment increased the bond value up to 1.34 MPa, and the results were compared with the bond strength of the deformed steel bar at 2.43 MPa. Based on the recent study, the best material that reduces moisture absorption and improves bamboo–concrete bonds is Sikadur-32 Gel. However, this coating material is costly to use as bamboo treatment. Another alternative that has been used is oil and bitumen-based material as a coating material, but these materials are not fully effective in the treatment of bamboo. Moreover, even though this material can reduce the bamboo swell–shrink activities, it can also impede the bamboo–concrete bond by decreasing the chemical adhesion and friction and acting as a lubricant between bamboo and concrete, especially when an ample amount is used. Thus, it is imperative and worthwhile to explore a new method to reduce the bamboo swell–shrink while increasing the bond performance of bamboo-reinforced concrete structures.

Previous studies focused on the treatment of bamboo surfaces, such as coating, instead of improving the concrete used on the bamboo-reinforced concrete. As the type of concrete can also affect the behavior of bamboo-reinforced concrete, a suitable concrete type should be used. In recent years, geopolymer technology has gained interest amongst researchers and industries. These technologies can provide comparable performance to or-

dinary Portland concrete in various applications as geopolymers are more environmentally friendly and have reduced greenhouse emissions [16,17]. Geopolymers can offer an enticing alternative to OPC binder in terms of environmental benefits to reduce carbon dioxide emissions. Not limited to that, geopolymer concrete also provides better performance and durability than OPC does. Due to similar or the same binding properties, geopolymers can be represented as an alternative to OPC [18]. The term "geopolymers" was coined by Joseph Davidovits in 1972 [19] to describe zeolite-like polymers. In the present day, terms such as "alkali-activated cement" [20], "inorganic polymer" [21], and "geocement" [22] are all used to describe material that is synthesized using the same chemistry. Geopolymers are aluminosilicate polymers that consist of three-dimensional amorphous monomers in a highly concentrated alkaline solution [23]. In order to induce the geopolymerization process, several binder materials that contain aluminosilicate from industrial waste, such as fly ash or slag, are used as raw materials in the production of geopolymer. Generally, the geopolymerization reaction consists of three primary steps: dissolution of aluminosilicate sources, gel formation, and setting or polycondensation [24].

Recently, geopolymers have increasingly gained interest due to their outstanding properties, including strength development, dense microstructures, low permeability, superior resistance to fire, and chemical resistance [24–26]. However, in terms of deterioration of the conventional bar, water or moisture absorbed by the concrete can lead to bar corrosion. When corrosion of the bars takes place, it results in microcracking and spalling of the concrete and eventually reduces the lifespan of the structures. No documented proof has shown that the bamboo deteriorated inside the concrete due to water or moisture in bamboo-reinforced concrete. However, the water or moisture absorbed by the concrete can cause microcracks due to the bamboo swell and shrink, mainly when OPC concrete is applied together in bamboo-reinforced concrete (see Figure 1). Luhar and Khandenwal [27] reported that the water absorption of the geopolymer is relatively low compared to OPC concrete. The advantage in terms of low water absorption also provides a basis for applying geopolymers in bamboo-reinforced concrete structures. However, current studies have focused on using geopolymer in conventional reinforced concrete structures [28,29].

(a) (b)

Figure 1. (**a**) Treatment of fresh bamboo culm; (**b**) completely treated bamboo culm.

According to the author's literature review, few studies on bamboo are related to geopolymers. Sá Ribeiro et al. conducted a study on the properties of a geopolymer-bamboo composite by incorporating bamboo fiber in the metakaolin geopolymer [30]. Another study on fly ash-based geopolymer concrete properties was carried out by incorporating bamboo ash under elevated temperatures [31]. However, most previous studies focused on the use of bamboo fiber and bamboo ash to produce either bamboo-composite products or geopolymer concrete. There was no information regarding the application of bamboo strips as reinforcement in geopolymer concrete structures. Bamboo strips and concrete bonds are the keys to ensuring that these two materials can work together in bamboo-reinforced geopolymer concrete structures. To fill this knowledge gap, the experimental study was carried out to investigate the bond performance of the bamboo strip embedded in FAG

concrete. In this study, a total of twenty-four pull-out specimens were cast, with three of the specimens cast in OPC concrete as control specimens, and the rest being cast in FAG concrete for comparison purposes. Furthermore, modifications of the bamboo strip were also created in light of the fact that the plain bamboo strip alone would not produce a significant bond strength, as reported in previous studies. The bond characteristic, the effect of concrete moisture, and the mode of failures are discussed in this paper.

2. Materials and Methods

2.1. Material Properties

2.1.1. Bamboo

Bamboo species of the *Bambusa vulgaris* (Buluh Minyak) from Sungai Siput, Perak, Malaysia, with an average length of each bamboo culm of 3 m, was used in this study. Two steps were involved in preparing bamboo: (a) selecting mature bamboo culms and (b) cleaning and preserving bamboo culms. In the preservation process, the soak diffusion method was used, in which all the bamboo was soaked in a mixture of boric acid and borax in a 1:1.5 ratio. The boric acid and borax come in a powder form, and the combination of both powders in this ratio forms an alkaline salt known as Disodium Octaborate Tetrahydrate. These powders were then diluted with water in a rectangular water tank where the 1:1.5 ratio is based on the weight of powders in kilograms per 100 L of water. The bamboo culms were then soaked into the water tank, and this preservation process took approximately one week, as shown in Figure 1a. The bamboo culms were then dried under the shed until the bamboo color changed to yellowish, as shown in Figure 1b. The purpose of the soak diffusion using boric acid and borax is to remove the starch and carbohydrates in the bamboo culm so that the resistance toward insect and microbial attack is increased. In addition, boric acid and borax were used in bamboo preservation because they are relatively cheap and have no adverse impact on humans if the proper dosage is used [32].

Prior to each testing, the bamboo culms were cut into strip form with a bamboo splitter and trimmed with a bamboo knife to obtain the desired dimensions. The bamboo strip was cut to an overall length and width of 260 mm and 20 mm for the tensile strength test, respectively. Meanwhile, the effective length and width were 65 mm and 10 mm, respectively, and the thickness of the tensile specimen was according to the bamboo thickness. Then, the moisture content specimen was cut into a prism shape with a dimension of 25 mm in width and height, while the thickness was according to the bamboo thickness. The tensile strength and moisture content tests were conducted according to ISO-22157-1 [33].

2.1.2. Concrete

There were two types of concrete mixes with a designed compressive strength of 40 MPa, which were Ordinary Portland cement concrete (OPCC) and fly ash geopolymer concrete (FAGC). The OPCC has the same constituent materials as FAGC except for the binder. An Ordinary Portland cement with a specific gravity of 3.14 was used in the production of OPCC, while a Class F fly ash was used in the production of FAGC. The chemical composition of OPC and fly ash was detected using X-ray fluorescence (XRF) and is tabulated in Table 1. Crushed aggregate with a nominal size of 10 mm and river sand were used as the coarse and fine aggregate, respectively. A naphthalene-based superplasticizer and extra water were added to the concrete mixture to improve the workability of the concrete.

Table 1. Chemical composition of fly ash and OPC determined by XRF.

	Chemical Composition (%)							
	SiO_2	Al_2O_3	Fe_2O_3	CaO	MgO	Na_2O	K_2O	LOI
FA	36.2	12.1	23.1	19.2	1.9	0.1	2.9	1.9
OPC	20.1	4.9	2.4	65.0	3.1	0.2	0.5	2.5

The alkali activator consisted of Na_2SiO_3 (sodium silicate), and NaOH (10 M sodium hydroxide) was used in the FAGC mixture. The ratio of alkaline solution (Na_2SiO_3 to NaOH) was 2.5 by mass, while the ratio of alkaline solution to binder (Na_2SiO_3 + NaOH to fly ash) was 0.4 by mass. The Na_2SiO_3 and NaOH were mixed at the required amount and cooled down under laboratory conditions for about 24 h before the concrete specimens could be cast.

Both OPCC and FAGC mixed designs are tabulated in Table 2. All the specimens were cast and cured following each designated curing condition. The OPCC specimens were cured with a wet gunny, whereas the FAGC specimens were cured at ambient temperature for 28 days. To measure the strength of the concrete, compressive strength and splitting tensile strength were determined on a cube with sides of 100 mm and a cylinder of 100 mm in diameter and 200 mm in height, respectively. In addition, to compare the change in environmental humidity, a water absorption test was conducted on the cube specimens.

Table 2. Mix proportion of FAGC and OPCC.

| | Mixture Proportions (kg/m^3) | | | | | | | |
	Fly Ash	OPC	Na$_2$SiO$_3$	NaOH	Water	Sand	Coarse Aggregate	SP
FAGC	428	-	123	49	13	720	1080	8.56
OPCC	-	432	-	-	233	965	700	-

2.2. Design of the Pull-Out Specimens

In this study, the pull-out test was carried out to investigate the bond strength of the bamboo strip embedded in OPCC and FAGC. The pull-out concrete specimens were cast in a 200 mm × 200 mm × 200 mm cube wooden mold. The bamboo culm was cut into strip form with a length of 450 mm, and the width was kept constant at 20 ± 1 mm to minimize the crushing effect caused by the machine grip. The thickness of the bamboo strip depended on its own thickness. The bamboo strip had an embedded length of 200 mm. Half of the embedded length was de-bonded using a section of polyvinyl chloride (PVC) to prevent concrete splitting failure, as shown in Figure 2. The internal gap between the bamboo strip and PVC pipe was covered with a sellotape to avoid the slurry from entering the PVC pipe during the concrete casting process.
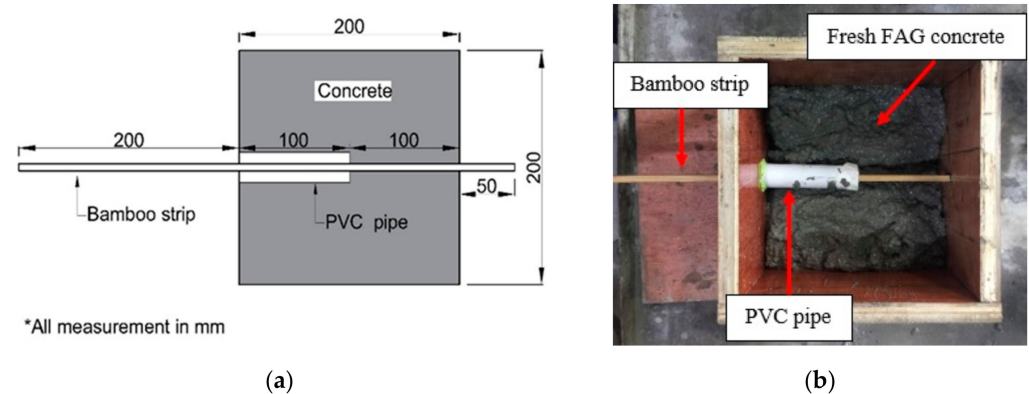

(**a**) (**b**)

Figure 2. (**a**) Geometry of bamboo pull-out specimen; (**b**) casting for pull-out specimen.

In this study, undeformed and deformed bamboo strips were compared to investigate further the mechanical interlocking effect on the bond strength of the bamboo embedded in concrete. The undeformed or natural state of the bamboo strip consisted of the bamboo strip with nodes and without nodes, as shown in Figure 3. Meanwhile, deformed bamboo strips had two types of deformation: corrugated and wrapped in galvanized iron (G.I) wire, as shown in Figure 4. The bamboo strips without nodes served as a control specimen.
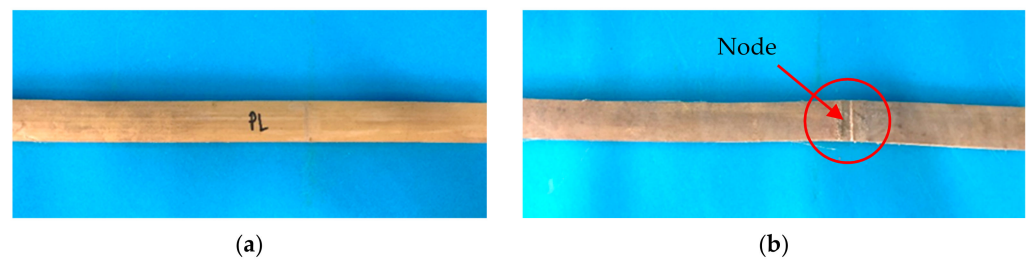
(a)   (b)

Figure 3. Undeformed bamboo strips (**a**) without nodes and (**b**) with nodes.
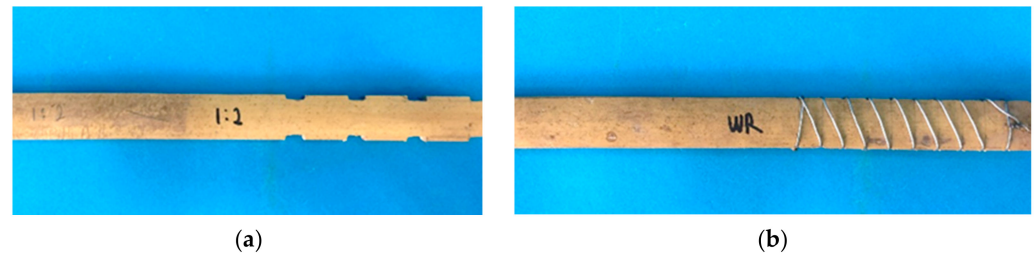

(a)   (b)

Figure 4. Deformed bamboo strips: (**a**) corrugated and (**b**) wrapped with G.I wire.

Corrugated bamboo strips were made by using a routing machine. The projection depth of the bamboo strips was fixed at 2 mm, as the previous study reported that the projection of 2 mm contributes to the highest bond strength. Moreover, the grooves were spaced apart to reduce their impact on the tensile strength of the splints. On the other hand, an increase in the projection depth will cause a reduction in the remaining depth and a decrease in the tensile area [34]. Meanwhile, the width of the grooves, A and B, were varied based on the ratio. The geometry and dimension of the corrugated bamboo strips are illustrated and tabulated in Figure 5a and Table 3, respectively.
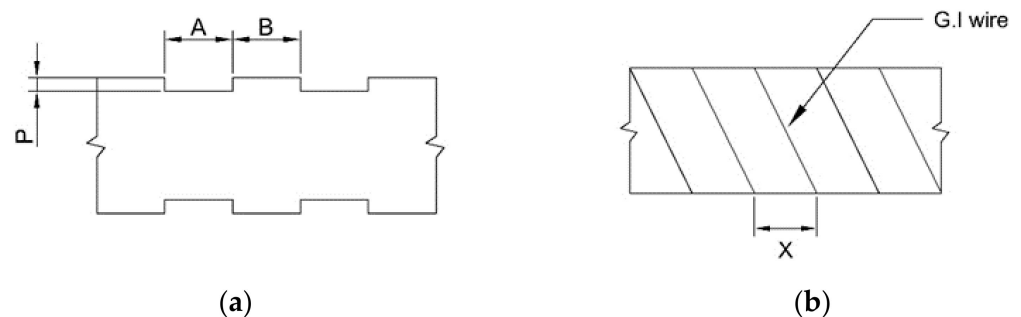

(a)   **(b)**

Figure 5. (**a**) Corrugated and (**b**) wired bamboo strip geometry.

Table 3. Dimension of corrugated bamboo strip.

Specimen	P (mm)	A (mm)	B (mm)	A:B
COR (1:1)	2	10	10	1:1
COR (1:2)	2	10	20	1:2

The second type of deformed bamboo strip was created by wrapping a bamboo strip with 0.8 ± 0.1 mm (diameter) Galvanized Iron (G.I) wire, as shown in Figure 5b. The size of G.I wire was chosen considering the availability in the local store. The bamboo strip was wrapped manually with G.I wire at 10, 20, and 30 mm spacing in a helical manner, as shown in Table 4. This method of upgrading the mechanical interlocking was chosen because it tends to have a more straightforward process and less energy needed to produce compared with the corrugated form. A total of 24 specimens were cast, with three specimens for

each type of bamboo strip. After the casting was complete, the specimens were kept in the laboratory for at least 24 h to allow the concrete to set before it could be demolded and cured according to their curing conditions.

Table 4. Dimension of wired bamboo.

Specimen	Spacing between G.I Wire, X (mm)
WR10	10
WR20	20
WR30	30

2.3. Pull-Out Loading Test Setup

The pull-out was carried out by adapting the RILEM RC6 Part 2 [35] on specimens at the age of 28 days. A Universal Testing Machine (Tinius Olsen Model 2000SL) with a capacity of 2000 kN was used to test the pull-out specimens, as shown in Figure 6. A special frame for the pull-out test was installed in the Universal Testing Machine to place the specimens. The specimen was turned upside down, with the longer bamboo strip facing down, and was clamped into the Universal Testing Machine grip. A steel plate was glued on the top of the specimen after it was positioned in the machine. The displacement was then measured using a Linear Variable Transducer (LVDT) pointed at the steel plate. A data logger was used to collect the pulling force and the displacement data at a controlled rate of 0.01 mm/s.
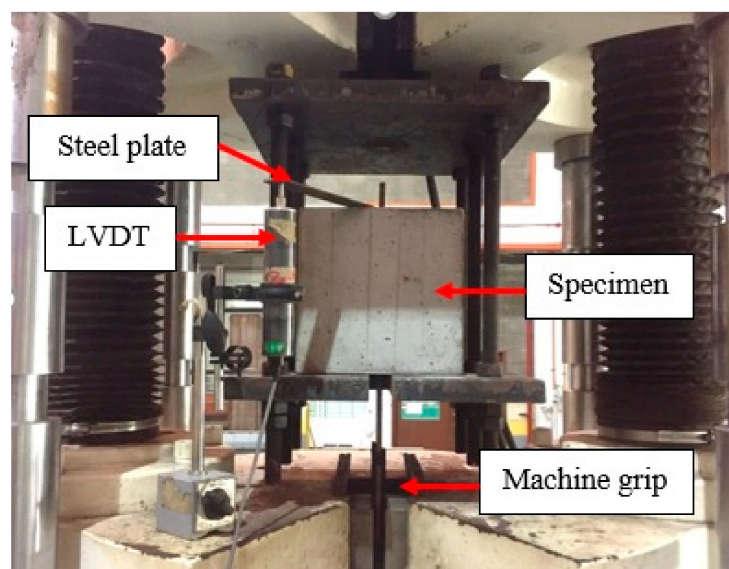

Figure 6. Pull-out test setup.

For each test, the type of failure was identified, and bond-stress results were recorded. The ultimate bond strength, τ, of the bamboo strip embedded in concrete was calculated using Equation (1) by assuming that the bond stress is evenly distributed along with the embedded length range.

$$\tau = \frac{P}{(2a + 2b)l} \tag{1}$$

where P represents the ultimate load applied (N), a is the width of the bamboo strip (mm), b is the thickness of the bamboo strip (mm), and l is the embedded length (mm).

3. Results and Discussion

3.1. Properties of Bambusa vulgaris and Concretes

Table 5 shows the properties of *Bambusa vulgaris* used in this study. From the tensile strength and moisture content test, the average tensile strength of the bamboo was in the range of 230 MPa to 320 MPa, with a moisture content range from 15% to 17%. Therefore, the tensile strength of the bamboo species used in this study can be categorized as a high-strength bamboo compared with other bamboo species available in Malaysia. This result is in agreement with a previous study conducted on the tensile strength of different bamboo species [36].

Table 5. Properties of bamboo *Bambusa vulgaris*.

Species	Tensile Strength (MPa)	Modulus of Elastic (GPa)	Average Moisture Content (%)
Bambusa vulgaris	230–320	30–38	15–17

Meanwhile, Table 6 shows the properties of FAGC and OPCC. The results showed that the slump value for FAGC was slightly lower than that of the OPCC. This may be due to the FAGC fresh mix having a higher viscosity than the OPCC fresh mix due to the use of Na_2SiO_3 and a high concentration of NaOH solution [37]. The compressive strength of FAGC was also slightly lower than that of the OPCC, with a difference of 1 MPa. The strength of FAGC could be higher if heat curing was applied in this study; however, ambient curing was applied considering the practicality and the amount of CaO in the fly ash. In the process of a chemical reaction in geopolymerization, heating is needed to initiate the chemical reaction in some cases. However, fly ash-based geopolymer with a CaO content of more than 8% does not need heating to initiate the reaction. It will generate heat to some degree that may later initiate the chemical reaction [38].

Table 6. Properties of concrete.

Concrete	Slump (mm)	f_{cu} (MPa)	f_{ct} (MPa)	Water Absorption (%)	Density (kg/m^3)
FAGC	84	40	3.8	1.34	2310
OPCC	145	41	3.1	3.52	2195

The results also showed that the water absorption of FAGC was lower than that of OPCC concrete. This low water absorption rate indicates restricted open porosity, which can prevent water from flowing freely into the concrete. In addition, the low water absorption possessed by FAGC may be attributed to the presence of silicate ions (Si), the formation of compacted structures in the geopolymer matrix system, and the completion of the geopolymerization process [39].

3.2. Bond Strength

Table 7 shows the bond strength, τ, of the different bamboo strips embedded in OPCC and FAGC, where PL (IN) denotes the bamboo strip without nodes and PL-(N) denotes the bamboo strip with nodes. "COR (1:1)" denotes the corrugated bamboo strip with a corrugation ratio of 1:1 and "COR (1:2)" denotes the corrugated bamboo strip with a corrugation ratio of 1:2. Lastly, WR10, WR20, and WR30 denote bamboo strips rolled with G.I wire at 10 mm, 20 mm, and 30 mm, respectively.

The control specimen OPCC-PL (IN) had the lowest average bond strength of 0.67 MPa, followed by FAGC-PL (IN), which had an average bond strength of 0.73 MPa, as shown in Table 6. These results were expected as the bamboo strip embedded in these specimens was a plain bamboo strip without the presence of nodes or any surface modification. On the other hand, FAGC-WR 10 achieved the highest average bond strength of 1.48 MPa. Therefore, in order to acquire a better insight into the effect of the different types of concrete

and bamboo strips on the bond strength of bamboo pull-out specimens, Figure 7 shows the bond strength increment of these specimens compared with the control specimen OPCC-PL (IN).

Table 7. The results of tested pull-out specimens.

| Specimen	Type of Concrete	Bond Strength (MPa)	Average Bond Strength (MPa)	Average Bond Strength Increment (%)	Failure Mode
OPCC-PL (IN)	Ordinary Portland cement	0.63			Pull-out
OPCC-PL (IN	Ordinary Portland cement	0.71	0.67	0	Pull-out
OPCC-PL (IN)	Ordinary Portland cement	0.67			Pull-out
FAGC-PL (IN)	Fly ash geopolymer	0.77			Pull-out
FAGC-PL (IN)	Fly ash geopolymer	0.70	0.73	9	Pull-out
FAGC-PL (IN)	Fly ash geopolymer	0.72			Pull-out
FAGC-PL (N)	Fly ash geopolymer	0.87			Pull-out
FAGC-PL (N)	Fly ash geopolymer	0.90	0.87	30	Pull-out
FAGC-PL (N)	Fly ash geopolymer	0.83			Pull-out
FAGC-COR (1:1)	Fly ash geopolymer	1.29			Pull-out
FAGC-COR (1:1)	Fly ash geopolymer	1.47	1.40	109	Pull-out
FAGC-COR (1:1)	Fly ash geopolymer	1.45			Pull-out
FAGC-COR (1:2)	Fly ash geopolymer	1.42			Pull-out
FAGC-COR (1:2)	Fly ash geopolymer	1.49	1.45	116	Pull-out
FAGC-COR (1:2)	Fly ash geopolymer	1.45			Pull-out
FAGC-WR10	Fly ash geopolymer	1.47			Pull-out
FAGC-WR10	Fly ash geopolymer	1.51	1.48	121	Pull-out
FAGC-WR10	Fly ash geopolymer	1.46			Pull-out
FAGC-WR20	Fly ash geopolymer	0.95			Pull-out
FAGC-WR20	Fly ash geopolymer	0.81	0.88	31	Pull-out
FAGC-WR20	Fly ash geopolymer	0.87			Pull-out
FAGC-WR30	Fly ash geopolymer	0.87			Pull-out
FAGC-WR30	Fly ash geopolymer	0.73	0.80	19	Pull-out
FAGC-WR30	Fly ash geopolymer	0.79			Pull-out
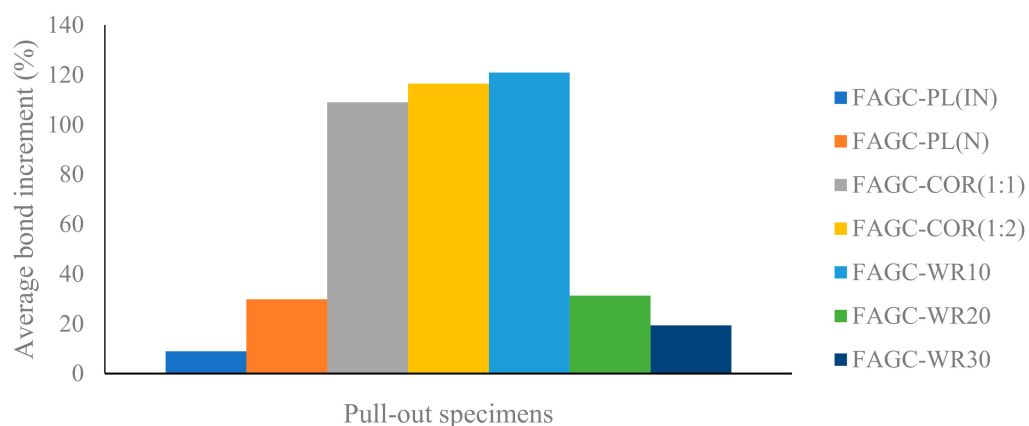
Figure 7. Average percentage of bond increment of all specimens as compared to the control, OPCC-PL(IN).

FAGC-PL (IN) specimens with a similar type of bamboo strip as the control specimen, OPCC-PL (IN), but a different type of concrete, showed a slight increase in the bond strength of about 9%. This may be attributed to the dense interfacial transition zone between the aggregates and the geopolymer binder, which improved the constraint force surrounding the bamboo strip. For FAGC-PL (N), the average bond increment was approximately 30%. The FAGC-PL (N) specimen's bond strength was higher than that of FAGC-PL (IN) due to the uneven surface conditions at the node part of the bamboo strip. The remaining diaphragm's presence at the inner part and rough surface conditions at the outer part of the bamboo strip contributed to the high mechanical interlock resistance. A significant difference in bond strength increment between FAGC-PL (IN) and FAGC-PL (N) specimens demonstrated that the geometry of the bamboo strip influenced the bond strength of the embedded bamboo strips. The small bonds increment shown by FAGC-PL (IN) proved that the plain bamboo strip could not develop a sufficient bond between the bamboo strip and adjoining concrete. In contrast, the bamboo strip in FAGC-PL (N) specimens demonstrated an acceptable bond behavior between the bamboo and the concrete matrix. This is due to the fact that the bamboo strip is dependent not only on the chemical adhesion and friction but also on the mechanical interlock developed by the presence of nodes.

Compared with OPCC-PL (IN), the FAGC-COR (1:2) specimens showed a more significant bond strength at the average bond increment of about 116%, which confirmed the corrugated effect on the bond strength. All the corrugated bamboo strips embedded in the concrete simultaneously had to result in the maximum mechanical resistance. The bond strength result of FAGC-COR (1:2) also showed that the 2 mm projection was large enough to develop a full mechanical interlock between the bamboo strip and the concrete surface. A similar observation was also reported by Khatib and Nounu [30].

Meanwhile, the FAGC-WR10 achieved the highest bond strength with an average bond strength of 1.48 MPa and bond increment of about 121%. In contrast, the different wire spacing shown by the companion specimens, which were FAGC-WR20 and FAGC-WR30, recorded small increments in bond strength of approximately 31% and 19%, respectively. This is due to the fact that the small spacing between wires wrapped around the bamboo strip in FAGC-WR10 provides a greater mechanical interlocking resistance than the companion specimens with larger spacing. Thus, the wire wrapped at 20 mm and 30 mm spacing did not contribute significantly to the bond between the bamboo strip and the concrete matrix.

3.3. Effect of Different Concrete on the Bamboo Moisture Content

It was known that moisture could affect the bond strength between bamboo and concrete. Generally, OPCC has a higher water content than FAGC. High water content in OPCC can reduce the bond strength of the embedded bamboo strip. When excessive water is added to the mixture, the bleed water also increases during the concrete consolidation. This will result in the formation of open pores between the reinforcement and the concrete [40]. In the FAGC mix, the water sources come from the alkaline solution. A small amount of water was added to the FAGC only to improve the workability of FAGC. In this study, the effect of concrete moisture on bond strength was evaluated by measuring the moisture content of the bamboo strips before and after the pull-out test.

As shown in Table 8, bamboo strips in the OPCC-PL (IN) specimen recorded the highest moisture increment at 26.11%. This is because OPCC had a high moisture content in its fresh state and was exposed to high humidity during the curing period. When the fresh OPCC was poured, the water in the fresh concrete moistened the bamboo strip. In addition, the OPCC-PL (IN) specimens were cured by the wet curing method using a wet gunny until the tested day. It was known that the water absorption of the OPCC was also high.

Table 8. The initial and final moisture content of bamboo strips.

Specimen	Average Initial Moisture Content (%)	Average Final Moisture Content (%)	Average Moisture Content Increment (%)
OPCC-PL (IN)	15.7	19.8	26.11
FAGC-PL (IN)	15.5	16.2	4.52
FAGC-PL (N)	15.4	16.2	5.19
FAGC-COR (1:1)	15.9	16.7	5.03
FAGC-COR (1:2)	15.9	16.6	4.40
FAGC-WR10	15.7	16.5	5.09
FAGC-WR20	16.0	16.8	5.00
FAGC-WR30	16.1	16.9	4.97

As bamboo is a hygroscopic material, it absorbs moisture from the surrounding environment. After the curing period, the OPCC will harden and lose water and cause the bamboo to dry out again. This drying process will lead to bond breakage between the bamboo strips and concrete as the bamboo strips swell and shrink [15]. Table 8 also shows that the moisture content increment was almost similar for all FAGC specimens that varied in the geometry of the bamboo strip. It was proven that the moisture content in the bamboo strip was influenced by the types of concrete used rather than the geometry of the bamboo strip.

However, it is worth mentioning that FAGC pull-out specimens' bond strength may also be reduced if too much water was added during the casting process. Increasing the amount of water added into the FAGC mixture can reduce the bond strength. The excess water added into the geopolymer concrete mixture leads to water evaporation from the concrete, thus leaving cavities and pores within the geopolymer matrix. Water evaporation rapidly occurs, especially when the geopolymer concrete is cured at high temperatures [41]. In the FAGC specimen in this research, the extra water added was very low, up to 3% of the total fly ash content, and, when mixed with the alkaline solution and fly ash, produced a viscous geopolymer concrete. As the ambient cured condition was applied to FAGC specimens, the amount of moisture from the concrete itself and the surrounding environment had been minimized, thus reducing the bond breakage caused by the swell and shrink of the bamboo strip.

3.4. Load–Slip Behavior

The performance and behavior of the pull-out load versus slip for bamboo specimens with different surface properties are discussed further in this section. The load and slip relationship represents the bond behavior between the bamboo strip and surrounding OPCC and FAGC. The displacement of the bamboo strip in the direction of the applied load from the adjoining concrete is measured as a slip. As shown in Figure 8, the bamboo specimen with G.I rolled wire of 10 mm spacing sustained a higher load and slip up to 8 mm before failing completely. After the specimen's failure at the highest load, the specimen experienced a plateau phase where the bamboo strip's slip increased steadily without increasing the load. This was possibly due to the ribbed action, which provided a mechanical interlock contributed by the closest spacing between the wire wrapped around the bamboo strip, which was absent in the plain bamboo specimen. The G.I wire was still intact with the bamboo strip during the pulling process, and it continuously provided ribbed action until it reached the higher load, thus explaining the higher slip compared with other specimens.
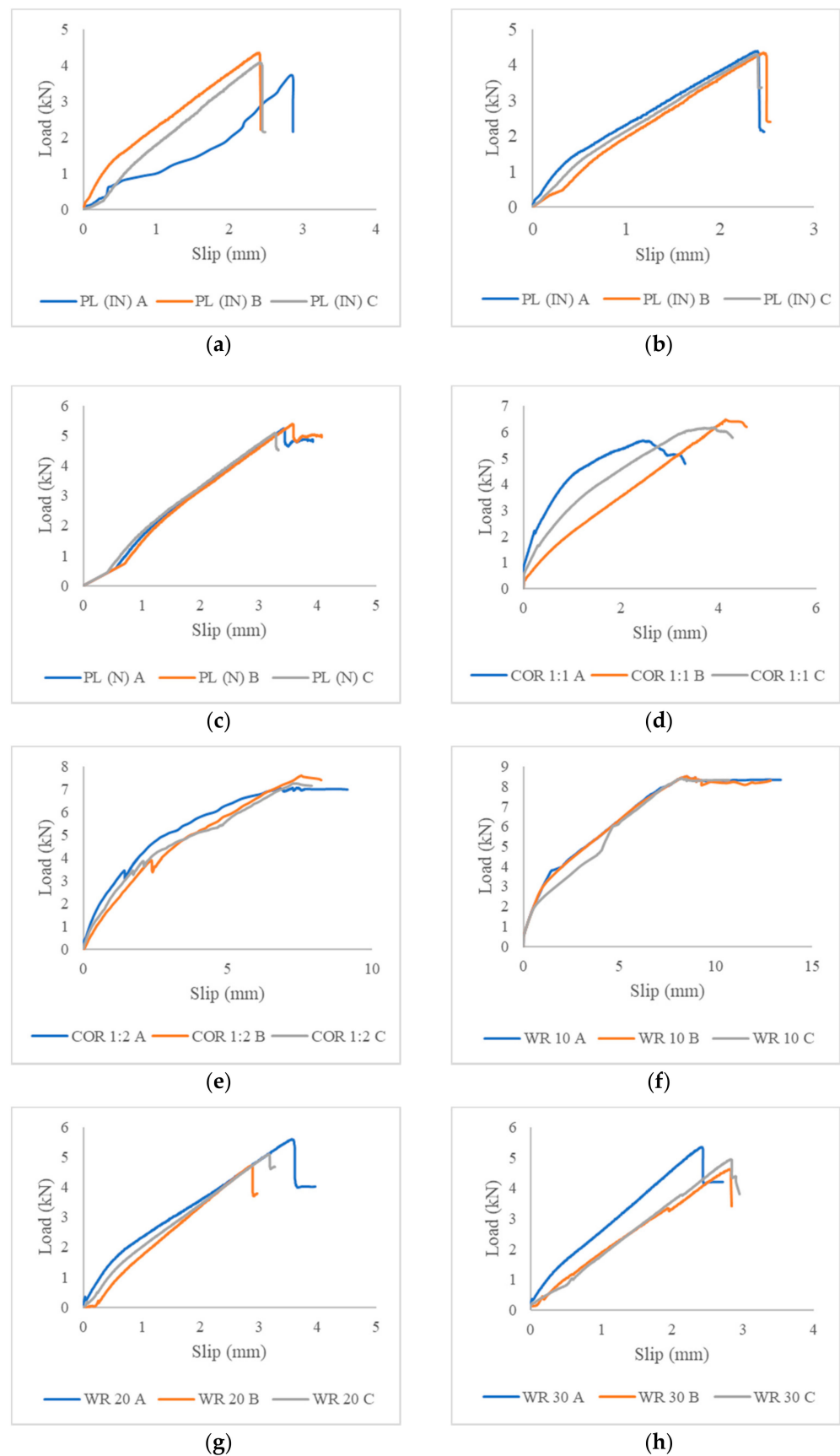
Figure 8. Load–slip curve of pull-out specimens: (**a**) OPCC-PL (IN), (**b**) FAGC-PL (IN), (**c**) FAGC-PL (N), (**d**) FAGC-COR (1:1), (**e**) FAGC-COR (1:2), (**f**) FAGC-WR10, (**g**) FAGC-WR20, and (**h**) FAGC-WR30.

Despite the fact that the bond strengths of FAGC-WR20 and FAGC-WR30 specimens were greater than those of undeformed bamboo specimens embedded in OPCC and FAGC, FAGC-WR20 and FAGC-WR30 showed a similar load–slip curve to those undeformed bamboo specimens. The specimens showed linear behavior as the bond between the bamboo strip with the adjoining concrete still existed until it completely diminished at the ultimate load and resulted in the curve moving downward after reaching the ultimate load. However, the load and the slip were lower than those of the bamboo specimen with G.I rolled wire of 10 mm spacing. This is because a higher G.I wire spacing provides a lower ribbed action, and as the load increases, the ribbed action is diminished when the ultimate bond stress is achieved. The load–slip curve of FAGC-WR20 and FAGC-WR30 specimens showed a linear elastic behavior until the ultimate load was reached. Then, the slipping of bamboo started, and the curve moved down gradually due to a complete failure before entering a plateau phase.

OPCC-PL (IN), FAGC-PL (IN), and FAGC-PL (N) specimens also had a similar curve trend as the FAGC-WR20 and FAGC-WR20 specimens. The pull-out load–slip showed a linear elastic behavior until the ultimate load was reached. The FAGC-COR (1:2) specimen also showed a similar curve trend as the FAGC-WR10 specimen. The FAGC-COR (1:2) specimen experienced a long slip before it failed and entered a plateau phase. The long slip experienced by the FAGC-COR (1:2) specimen may be due to the interlocking effect that still existed during the pulling process. The grooves on the bamboo strips were still intact, thus giving a higher resistance with a longer slip. Meanwhile, FAGC-COR (1:1) specimen showed a similar curve trend to the FAGC-WR20, FAGC-WR30, and undeformed bamboo specimens, with the exception that the curve at the linear part was steeper than those of the other specimens.

3.5. Mode of Failure

To observe the bond failure between the bamboo strip and concrete interface, the specimen was dissected. The pull-out failure was identified for all the bamboo specimens during the pull-out test. Generally, an undeformed or plain bamboo strip does not develop enough anchorage bond to the concrete matrix. In contrast, deformed bamboo strips such as corrugated and wired bamboo can develop an anchorage bond using its ribs, which, in this case, were provided by the grooves and the wire wrapped around the bamboo strips. As shown in Figure 9, when the plain bamboo strip was under pull-out loading, the smooth bamboo strip surfaces generated a frictional force reaction with the adjoining concrete. However, deformed bamboo strips produced additional bearing forces, which were resisted by the concrete, thus generating the interlocking effect. As the pull-out failure of the bamboo strip was determined, no crack appeared on the concrete surface when the bamboo strip was slowly pulled out from the concrete block during the pull-out procedure. Therefore, in the case of bamboo strips pulled from the concrete, the forces that existed induced by the mechanical interlock were not strong enough to develop cracks in the concrete matrix.

The pull-out failure was identified for the plain bamboo strip taken from the internode part, as the plain bamboo surface provided minimum resistance to the bamboo–concrete interface. The pull-out or slippage of the bamboo strip can be explained in a straightforward mechanism. When the pull-out force goes beyond the friction forces instead of the tensile capacity of the bamboo strip, the bar will completely slip from the concrete cube [11]. Figure 10a,b show that the plain bamboo strip at the internode part left a smooth track at the OPCC and FAGC surface. Meanwhile, Figure 10c shows the exfoliation marks of the bamboo node at the concrete surface. The exfoliation mark indicates that the irregular forms in the node contributed to the enhancement of the mechanical resistance toward the concrete surface before failing in pull-out.
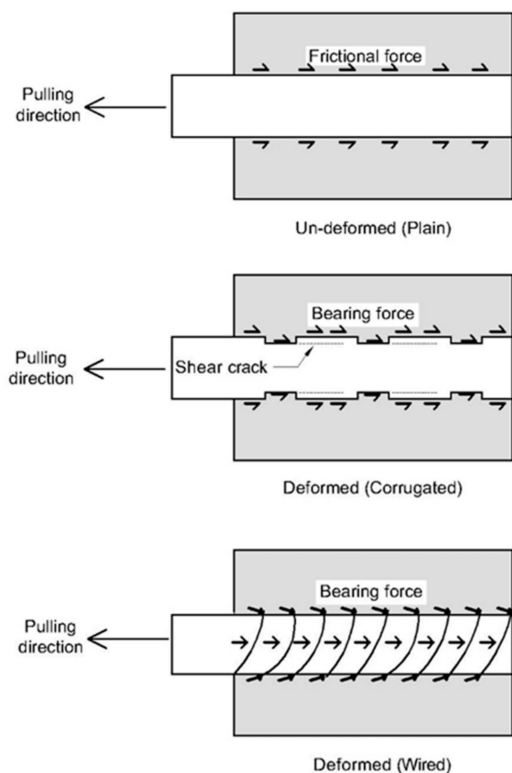
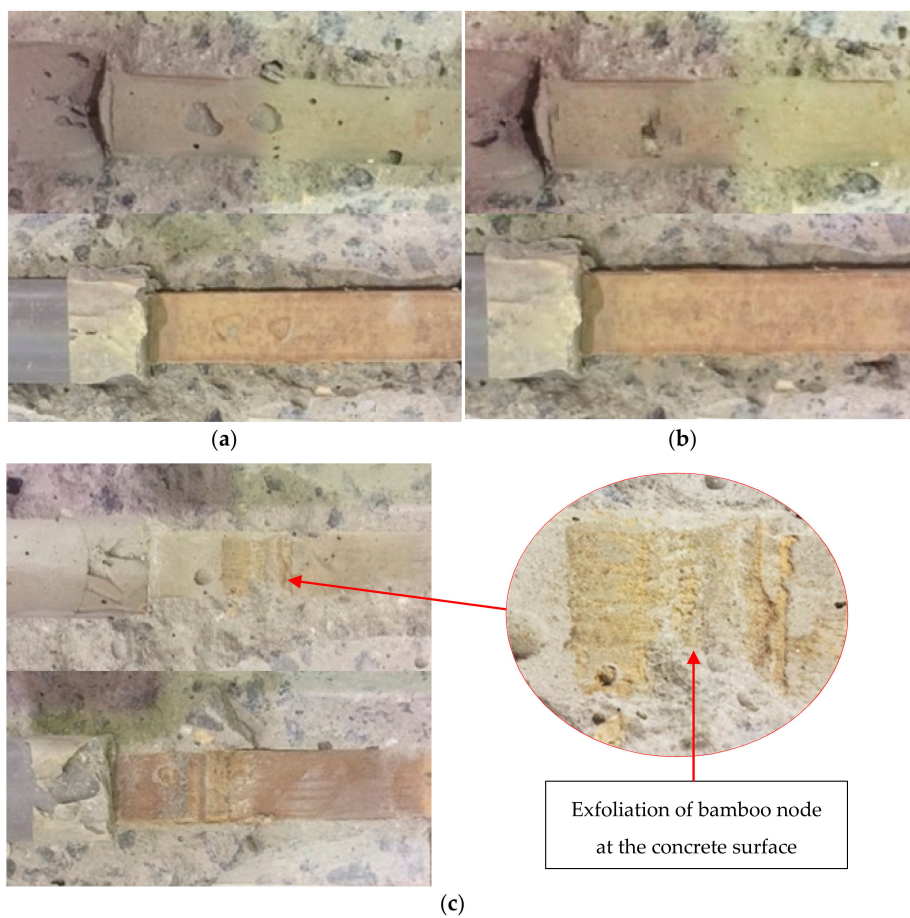**Figure 9.** General pull-out mechanisms of bamboo strips.

(**a**)　　　　　　　　　　　　　　(**b**)

(**c**)

Exfoliation of bamboo node at the concrete surface

Figure 10. Failure patterns of plain bamboo strip: (**a**) OPCC-PL (IN), (**b**) FAGC-PL (IN), and (**c**) FAGC-PL (N).

Figure 11a shows the corrugated bamboo strip with a 1:1 ratio after extracting from the FAG concrete block. It can be observed that most of the corrugated bamboo strips were severely damaged and sheared-off along the bamboo strip after the completion of the pull-out test. The shearing of the bamboo can cause the failure between the corrugated bamboo and the adjoining concrete, as well as the shearing of the concrete between the corrugated bamboo strips. In addition, it also can weaken the mechanical interlock due to shrinkage and by the mechanical properties of bamboo in the direction perpendicular to fibers, as it can be easily compressible compared with steel or concrete. The sheared-off corrugated bamboo strip indicates that the shear resistance of the bamboo strip at a 1:1 ratio was weaker than that of the concrete strength. Moreover, the sheared-off bamboo occurred because the concrete shear strength overcame the longitudinal shear strength of bamboo along with the fiber. Meanwhile, the corrugated bamboo strip with a 1:2 ratio showed few undamaged corrugated parts along the bamboo strip, indicating partial corrugated failure, as shown in Figure 11b. From the failure shown by the corrugated bamboo specimens, it can be concluded that an adequate bonding was established at the bamboo strip and concrete surface. The damaged and sheared-off corrugated bamboo strips also indicated their participation in resisting the pull-out load [42].
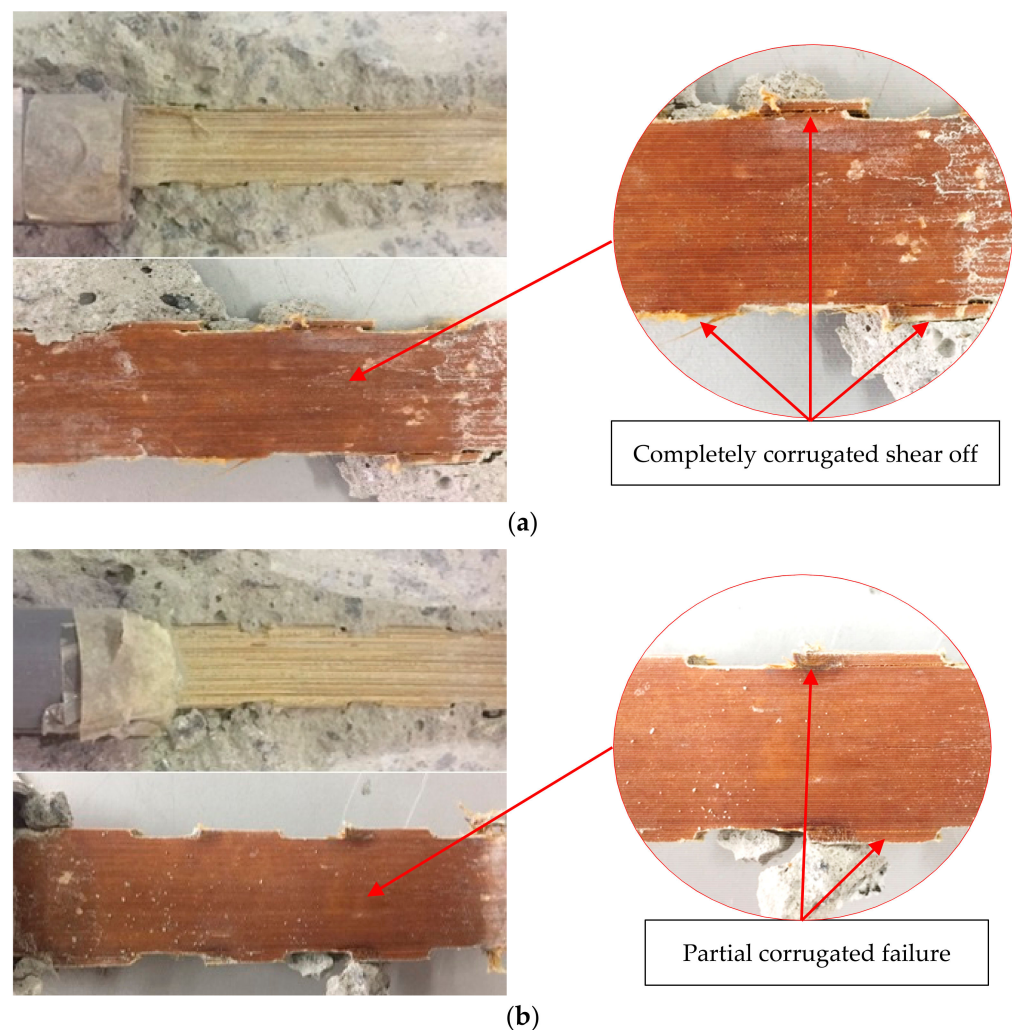

Completely corrugated shear off

(**a**)

Partial corrugated failure

(**b**)

Figure 11. Failure patterns of corrugated bamboo strip: (**a**) FAGC-COR2 (1:1) and (**b**) FAGC-COR2 (1:2).

Meanwhile, the mode of failure shown by the bamboo specimens wrapped with wire was different from the other bamboo forms. After dissection, the cross-section of the FAGC indicated an intact wire rib mark at the surface of the FAGC and bamboo specimen with

wire. The entire wire rib marks existed in all bamboo specimens wrapped with wire. However, the large deformation of a wire wrapped around the bamboo strip was shown by the specimen FAGC-WR10. It was noticed that the wire wrapped at a 10 mm distance changed significantly, where the wire was likely being pulled out from its original position by the friction between the concrete surface and the bamboo strip (see Figure 12a). The deformation of wire shown by the specimen FAGC-WR10 indicated the participation of wire in the pulling process. The closer wire wrapped around the bamboo strip increased the resistance and friction between the bamboo and concrete surfaces.
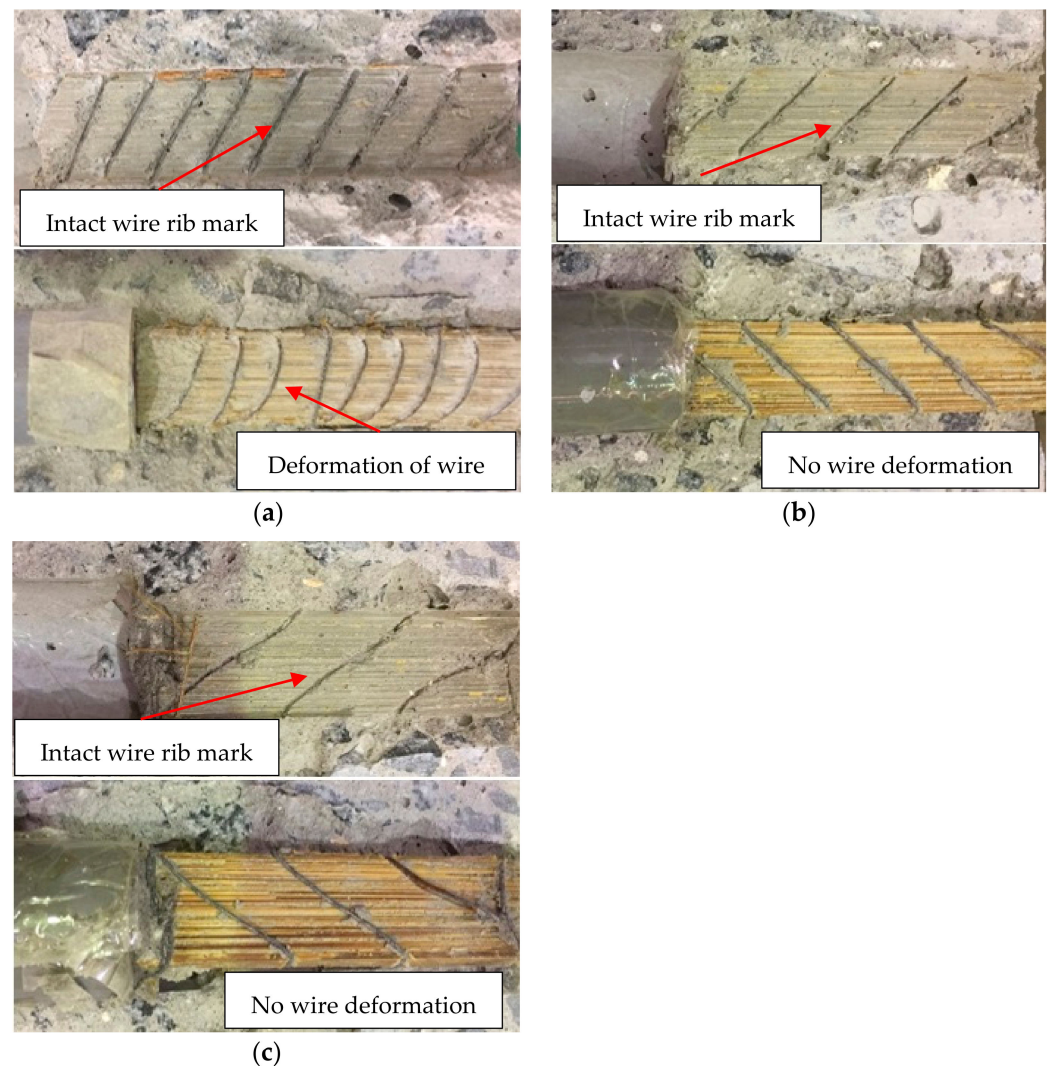
Figure 12. Failure patterns of wired bamboo strip: (**a**) FAGC-WR10, (**b**) FAGC-WR20, and (**c**) FAGC-WR30.

Other specimens with 20 mm and 30 mm wire distance did not show any deformation on the wire wrapped around the bamboo strip, as shown in Figure 12b,c. The wire wrapped around the bamboo strip was observed to remain maintained at its original position. The unchanged wire position indicated the only small contribution of wire to resist the pull-out force. This also explained why the pull-out strengths of FAGC-WR20 and FAGC-WR30 specimens were very low compared with FAGC-WR10 specimens.

4. Conclusions

In this study, the pull-out test was conducted to evaluate the effect of bamboo strip geometry and concrete type on the bond behavior of the bamboo strip embedded in concrete. Based on the experimental results and discussion that has been presented, the following conclusions can be drawn.

1. The modification of the surface of the bamboo strip increased the bond strength. The highest bond strength was showed by the wired bamboo form (10 mm) and followed by the corrugated form (1:2). The mechanical adhesion provided by the rolled wire and corrugated form increased the bamboo–concrete bond compared with plain bamboo, which relies on friction and chemical adhesion only.
2. For plain bamboo strips, the pull-out behavior was controlled by the bond physical and chemical component, whereas in the deformed bamboo strip, it was controlled by its mechanical interlock.
3. The bamboo strips embedded in the concrete failed in pull-out even though the modification of the strip was made. For corrugated specimens, the grooves were slightly deteriorated, which demonstrates their participation in resisting the pull-out forces. The bamboo wrapped with G.I wire also showed a deformation on the position of the wire, which indicated similar resistance toward the pull-out forces.
4. FAGC contributed to the increment in the bond strength between bamboo and surrounding concrete. In addition, the properties exhibited by the FAGC, such as high density, low water absorption, and cured under ambient conditions, can reduce the moisture absorption by the bamboo strip; hence, the bond breakage may also be minimized.

Moreover, the long-term bonding behavior of bamboo embedded in geopolymer concrete against aggressive environments, including acidic rain and exposure to sunlight, is the subject of ongoing study.

References

1. Andonian, R.; Mai, Y.W.; Cotterell, B. Strength and Fracture Properties of Cellulose Fibre-Reinforced Cement Composites. *Int. J. Cem. Compos.* **1979**, *1*, 151–158.
2. Kamkam, C. The Influence of Palm Stalk Fiber-Reinforcement on the Shrinkage Stresses in Concrete. *J. Ferrocem.* **1994**, *24*, 249–254.

3.　Mansur, M.A.; Aziz, M.A. A Study of Jute Fibre Reinforced Cement Composites. *Int. J. Cem. Compos. Light. Concr.* **1982**, *4*, 75–82. [CrossRef]

4.　Kankam, C.K. Raffia Palm-Reinforced Concrete Beams. *Mater. Struct.* **1997**, *30*, 313–316. [CrossRef]

5.　Wang, Y.; Chen, J.; Wang, D.; Ye, F.; He, Y.; Hu, Z.; Zhao, G. A Systematic Review on the Composition, Storage, Processing of Bamboo Shoots: Focusing the Nutritional and Functional Benefits. *J. Funct. Foods* **2020**, *71*, 104015. [CrossRef]

6.　Huang, Z.; Zhong, X.J.; He, J.; Jin, S.H.; Guo, H.D.; Yu, X.F.; Zhou, Y.J.; Li, X.; Ma, M.D.; Chen, Q.B.; et al. Genome-Wide Identification, Characterization, and Stress-Responsive Expression Profiling of Genes Encoding LEA (Late Embryogenesis Abundant) Proteins in Moso Bamboo (*Phyllostachys edulis*). *PLoS ONE* **2016**, *11*, e0165953. [CrossRef]

7.　Jit Kaur, P. Bamboo Availability and Utilization Potential as a Building Material. *For. Res. Eng. Int. J.* **2018**, *2*, 8–11. [CrossRef]

8.　Liese, W. Research on Bamboo. *Wood Sci. Technol.* **1987**, *21*, 189–209.

9.　Shao, Z.P.; Fang, C.H.; Huang, S.X.; Tian, G.L. Tensile Properties of Moso Bamboo (*Phyllostachys pubescens*) and Its Components with Respect to Its Fiber-Reinforced Composite Structure. *Wood Sci. Technol.* **2010**, *44*, 655–666. [CrossRef]

10.　Glenn, H.E. *Bamboo Reinforcement in Portland Cement Concrete*; Engineering Experiment Station: College Station, TX, USA, 1950.

11.　Javadian, A.; Wielopolski, M.; Smith, I.F.C.; Hebel, D.E. Bond-Behavior Study of Newly Developed Bamboo-Composite Reinforcement in Concrete. *Constr. Build. Mater.* **2016**, *122*, 110–117. [CrossRef]

12.　Ghavami, K. Bamboo as Reinforcement in Structural Concrete Elements. *Cem. Concr. Compos.* **2005**, *27*, 637–649. [CrossRef]

13.　Agarwal, A.; Nanda, B.; Maity, D. Experimental Investigation on Chemically Treated Bamboo Reinforced Concrete Beams and Columns. *Comput. Chem. Eng.* **2014**, *71*, 610–617. [CrossRef]

14.　Ghavami, K. Ultimate Load Behaviour of Bamboo-Reinforced Lightweight Concrete Beams. *Cem. Concr. Compos.* **1995**, *17*, 281–288. [CrossRef]

15.　Terai, M.; Minami, K. Research and Development on Bamboo Reinforced Concrete Structure. *World Conf. Earthq. Eng.* **2012**, *15*, 1–10.

16.　Fernández-Jiménez, A.; Palomo, A. Mid-Infrared Spectroscopic Studies of Alkali-Activated Fly Ash Structure. *Microporous Mesoporous Mater.* **2005**, *86*, 207–214. [CrossRef]

17.　Bakharev, T. Thermal Behaviour of Geopolymers Prepared Using Class F Fly Ash and Elevated Temperature Curing. *Cem. Concr. Res.* **2006**, *36*, 1134–1147. [CrossRef]

18.　Pacheco-Torgal, F.; Castro-Gomes, J.; Jalali, S. Alkali-Activated Binders: A Review. Part 2. About Materials and Binders Manufacture. *Constr. Build. Mater.* **2008**, *22*, 1315–1322. [CrossRef]

19.　Komnitsas, K.; Zaharaki, D. Geopolymerisation: A Review and Prospects for the Minerals Industry. *Miner. Eng.* **2007**, *20*, 1261–1277. [CrossRef]

20.　Palomo, A.; López dela Fuente, J.I. Alkali-Activated Cementitous Materials: Alternative Matrices for the Immobilisation of Hazardous Wastes—Part I. Stabilisation of Boron. *Cem. Concr. Res.* **2003**, *33*, 281–288. [CrossRef]

21.　Sofi, M.; van Deventer, J.S.J.; Mendis, P.A.; Lukey, G.C. Engineering Properties of Inorganic Polymer Concretes (IPCs). *Cem. Concr. Res.* **2007**, *37*, 251–257. [CrossRef]

22.　Krivenko, P.V.; Kovalchuk, G.Y. Directed Synthesis of Alkaline Aluminosilicate Minerals in a Geocement Matrix. *J. Mater. Sci.* **2007**, *42*, 2944–2952. [CrossRef]

23.　Rowles, M.; O'Connor, B. Chemical Optimisation of the Compressive Strength of Aluminosilicate Geopolymers Synthesised by Sodium Silicate Activation of Metakaolinite. *J. Mater. Chem.* **2003**, *13*, 1161–1165. [CrossRef]

24.　Duxson, P.; Fernández-Jiménez, A.; Provis, J.L.; Lukey, G.C.; Palomo, A.; Van Deventer, J.S.J. Geopolymer Technology: The Current State of the Art. *J. Mater. Sci.* **2007**, *42*, 2917–2933. [CrossRef]

25.　Kong, D.L.Y.; Sanjayan, J.G.; Sagoe-Crentsil, K. Factors Affecting the Performance of Metakaolin Geopolymers Exposed to Elevated Temperatures. *J. Mater. Sci.* **2008**, *43*, 824–831. [CrossRef]

26.　Mesgari, S.; Akbarnezhad, A.; Xiao, J.Z. Recycled Geopolymer Aggregates as Coarse Aggregates for Portland Cement Concrete and Geopolymer Concrete: Effects on Mechanical Properties. *Constr. Build. Mater.* **2020**, *236*, 117571. [CrossRef]

27.　Luhar, S.; Khandelwal, U. A Study on Water Absorption and Sorptivity of Geopolymer Concrete. *Int. J. Civ. Eng.* **2015**, *2*, 1–9. [CrossRef]

28.　Maranan, G.B.; Manalo, A.C.; Karunasena, W.; Benmokrane, B. Pullout Behaviour of GFRP Bars with Anchor Head in Geopolymer Concrete. *Compos. Struct.* **2015**, *132*, 1113–1121. [CrossRef]

29.　Avirneni, D.; Peddinti, P.R.T.; Saride, S. Durability and Long Term Performance of Geopolymer Stabilized Reclaimed Asphalt Pavement Base Courses. *Constr. Build. Mater.* **2016**, *121*, 198–209. [CrossRef]

30.　Sá Ribeiro, R.A.; Sá Ribeiro, M.G.; Sankar, K.; Kriven, W.M. Geopolymer-Bamboo Composite—A Novel Sustainable Construction Material. *Constr. Build. Mater.* **2016**, *123*, 501–507. [CrossRef]

31.　Ishak, S.; Lee, H.S.; Singh, J.K.; Ariffin, M.A.M.; Lim, N.H.A.S.; Yang, H.M. Performance of Fly Ash Geopolymer Concrete Incorporating Bamboo Ash at Elevated Temperature. *Materials* **2019**, *12*, 3404. [CrossRef]

32.　Fattah, A.R.; Prinindya, K.N.N.; Ardhyananta, H. The Effect of Chemical Substance and Immersion Time to Tensile Strength of Bamboo Betung (Dendrocalamus Asper) as Chemical Preservation Treatment. *IPTEK J. Proc. Ser.* **2014**, *1*, 119–124. [CrossRef]

33.　International Organization for Standardization. *ISO 22157-1:2004*; Bamboo—Determination of Physical and Mechanical Properties—Part 1: Requirements; International Organization for Standardization: Geneva, Switzerland, 2004. [CrossRef]

34.　Khatib, A.; Nounu, G. Corrugated Bamboo as Reinforcement in Concrete. *Struct. Build.* **2017**, *170*, 311–318. [CrossRef]

35. RILEM. *RC 6 Bond Test for Reinforcement Steel.2. Pull-Out Test, 1983*; The International Union of Laboratories and Experts in Construction Materials, Systems and Structures: Paris, France, 1994.

36. Awalluddin, D.; Ariffin, M.A.M.; Zamri, N.F.; Ahmad, Y.; Ibrahim, I.S.; Osman, M.H.; Lee, H.S. Tensile and Shear Strength of Four Species of Bamboo in Malaysia. *IOP Conf. Ser. Mater. Sci. Eng.* **2020**, *849*, 012041. [CrossRef]

37. Memon, F.A.; Nuruddin, M.F.; Khan, S.; Shafiq, N.; Ayub, T. Effect of Sodium Hydroxide Concentration on Fresh Properties and Compressive Strength of Self-Compacting Geopolymer Concrete. *J. Eng. Sci. Technol.* **2013**, *8*, 44–56.

38. Wattimena, O.K.; Antoni; Hardjito, D. A Review on the Effect of Fly Ash Characteristics and Their Variations on the Synthesis of Fly Ash Based Geopolymer. *AIP Conf. Proc.* **2017**, *1887*, 020041. [CrossRef]

39. Duxson, P.; Provis, J.L.; Lukey, G.C.; Mallicoat, S.W.; Kriven, W.M.; van Deventer, J.S.J. Understanding the relationship between geopolymer composition, microstructure and mechanical properties. *Colloids Surf. A Physicochem. Eng. Asp.* **2005**, *269*, 47–58. [CrossRef]

40. Yan, H.; Kodur, V.; Liang, S.; Wu, B. Cement & Concrete Composites Characterizing the Bond Strength of Geopolymers at Ambient and Elevated Temperatures. *Cem. Concr. Compos.* **2015**, *58*, 40–49.

41. Al-Azzawi, M.; Yu, T.; Hadi, M.N.S. Factors Affecting the Bond Strength between the Fly Ash-Based Geopolymer Concrete and Steel Reinforcement. *Structures* **2018**, *14*, 262–272. [CrossRef]

42. Mali, P.R.; Datta, D. Experimental Study on Improving Bamboo Concrete Bond Strength. *Adv. Concr. Constr.* **2019**, *7*, 191–201. [CrossRef]